Acousto-optic interaction in polyimide coated optical fibers with flexural waves

E. P. ALCUSA-SÁEZ,[1] A. DÍEZ,[1,*] E. RIVERA-PÉREZ,[1] W. MARGULIS,[2,3] L. NORIN,[2,3] M. V. ANDRÉS[1]

[1]*Departamento de Física Aplicada y Electromagnetismo-ICMUV, Dr. Moliner 50, 46100 Burjassot, Spain*
[2]*Department of Fiber Photonics, Acreo AB, Electrum 236, 16440, Kista, Sweden.*
[3]*Department of Applied Physics, Royal Institute of Technology, Roslagstullsbacken 21, 10691 Stockholm, Sweden.*
**antonio.diez@uv.es*

Abstract: Acousto-optic coupling in polyimide-coated single-mode optical fibers using flexural elastic waves is demonstrated. The effect of the polyimide coating on the acousto-optic interaction process is analyzed in detailed. Theoretical and experimental results are in good agreement. Although the elastic attenuation is significant, we show that acousto-optic coupling can be produced with a reasonably good efficiency. To our knowledge, it is the first experimental demonstration of acousto-optic coupling in optical fibers with robust protective coating.

OCIS codes: (060.2310) Fiber optics; (230.1040) Acousto-optical devices.

References and links

1. B. Y. Kim, J. N. Blake, H. E. Engan, and H. J. Shaw, "All-fiber acousto-optic frequency shifter," Opt. Lett. **11**(6), 389-391 (1986).
2. D. Östling and H. E. Engan, "Narrow-band acousto-optic tunable filtering in a two-mode fiber," Opt. Lett. **20** (11), 1247–1249 (1995).
3. H. S. Kim, S. H. Yun, I. K. Kwang, and B. Y. Kim, "All-fiber acousto-optic tunable notch filter with electronically controllable spectral profile," Opt. Lett. **22**(19), 1476–1478 (1997).
4. T. A. Birks, P. S. Russell, and D. O. Culverhouse, "The acousto-optic effect in single-mode fiber tapers and couplers," J. Lightwave Technol. **14**(11), 2519–2529 (1996).
5. K. J. Lee, H. C. Park, B. Y. Kim, "Highly efficient all-fiber tunable polarization filter using torsional acoustic waves," Opt. Express **15**(19), 12362–12367 (2007).
6. A. Díez, T. A. Birks, W. H. Reeves, B. J. Mangan, and P. St. J. Russell, "Excitation of cladding modes in photonic crystal fibers by flexural acoustic waves," Opt. Lett. **25**(20), 1499–1501 (2000).
7. M. W. Haakestad and H. E. Engan, "Acoustooptic properties of a weakly multimode solid core photonic crystal fiber," J. Lightwave Technol. **24**(2), 838–845 (2006).
8. E. P. Alcusa-Sáez, A. Díez, M. González-Herráez, and M. V. Andrés, "Time-resolved acousto-optic interaction in single-mode optical fibers: characterization of axial nonuniformities at the nanometer scale," Opt. Lett. **39**(6), 1437-1440 (2014).
9. B. Stiller, S. M. Foaleng, J.-C. Beugnot, M. W. Lee, M. Delqué, G. Bouwmans, A. Kudlinski, L. Thévenaz, H. Maillotte, and T. Sylvestre, "Photonic crystal fiber mapping using Brillouin echoes distributed sensing," Opt. Express **18**(19), 20136-20142 (2010).
10. E. P. Alcusa-Sáez, A. Díez, and M. V. Andrés, "Accurate mode characterization of two-mode optical fibers by in-fiber acousto-optics," Opt. Express **24**(5), 4899-4905 (2016).
11. W. Zhang, L. Huang, K. Wei, P. Li, B. Jiang, D. Mao, F. Gao, T. Mei, G. Zhang and J. Zhao, "Cylindrical vector beam generation in fiber with mode selectivity and wavelength tunability over broadband by acoustic flexural wave." Opt. Express **24**(10), 10376-10384 (2016).
12. L. Carrión-Higueras, E. P. Alcusa-Sáez, A. Díez, M. V. Andrés, "All-fiber laser with intracavity acousto-optic dynamic mode converter for efficient generation of radially polarized cylindrical vector beams," IEEE Photonics J., **9**(1), 1500507 (2017).
13. T. Wei, "The Effects of Polymer Coatings on the Strength and Fatigue Properties of Optical Fibers," *Proceedings of the American Ceramics Society*, Chicago, IL, (April 1986).
14. Du-Ri Song, Chang Su Jun, Sun Do Lim, and Byoung Yoon Kim, "Effect of metal coating in all-fiber acousto-optic tunable filter using torsional wave," Opt. Express **22**(25), 30873–30881 (2014).

15. Ph. M. Nellen, P. Mauron, A. Frank, U. Sennhauser, K. Bohnert, P. Pequignot, P. Bodor, H. Brändle, "Reliability of fiber Bragg grating based sensors for downhole applications," Sens. Actuator A-Phys, **103**, 364-376 (2003).
16. D. K. Nath, G. W. Nelson, S. E. Griffin, C. T. Harrington, Y. He, L. J. Reinhart, D. C. Paine, and T. F. Morse, "Polyimide coated embedded optical fiber sensors," Proc. SPIE **1489**, 17–32 (1991).
17. W. Zhang, L. Huang, K. Wei, P. Li, B. Jiang, D. Mao, F. Gao, T. Mei, G. Zhang and J. Zhao, "Cylindrical vector beam generation in fiber with mode selectivity and wavelength tunability over broadband by acoustic flexural wave." Opt. Express **24**, 10376-10384 (2016).
18. M. V. Andres, M. J. Tudor, and K. W. H. Foulds, "Analysis of an interferometric optical fibre detection technique applied to silicon vibrating sensors," Electron. Lett. **23**, 774 (1987).
19. R. N. Thurston, "Elastic waves in rods and clad rods," J. Acoust. Soc. Am. **64**(1), 1-37 (1978).
20. A. W. Snyder and J. Jove, *Optical Waveguide Theory* (Springer, 1983).

1. Introduction

An acoustic/elastic wave propagating along an optical fiber has the capability to produce coupling between co-propagating optical fiber modes. Over the last decades, a variety of all-fiber, dynamic, and reconfigurable components based on this effect have been demonstrated. Using flexural, longitudinal, or torsional elastic modes, all-fiber frequency shifters, tunable filters, and switches have been reported [1-5]. Additionally, acousto-optic coupling has also been exploited as a technique for fine characterization of optical fibers [6-10] and for cylindrical vector beams generation [11-12].

From the practical point of view, the main limitation of fiber devices based on acousto-optic interaction arises from the huge elastic attenuation in fibers with standard protective acrylate coating. Consequently, the coating of the fiber section along which the acousto-optic interaction takes place must be removed. The bare fiber section compromises the long-term reliability of the fiber component. The combination of moisture and stress can cause microscopic flaws in the glass to propagate, resulting in fiber failure [13]. Recently, acousto-optic coupling using torsional waves was demonstrated in a thin metal-coated optical fiber [14]. The metal coating, in the order of a hundred nm thick, provides low attenuation of the elastic wave and surface protection of the fiber, but still fiber handling is compromised.

In this paper, we present the first experimental demonstration of in-fiber acousto-optic coupling in polyimide-coated single-mode optical fibers. Polyimide coated fibers feature high temperature operation (up to 300 ºC) and are typically designed for use in harsh environments [15]. They are particularly suited for embedded and high temperature applications [16]. Polyimide offers fiber protection with a thickness of just few microns. The relatively thin coating, high adhesion to the glass, and lower viscosity of polyimide coatings compared with conventional acrylate coatings contribute to reduce the damping of the elastic wave. Here, we present an experimental study of acousto-optic coupling in polyimide-coated single-mode optical fibers using flexural elastic waves. We show that mode coupling can be realized with good efficiency. The effect of the coating on the acousto-optic interaction process is analyzed in detail.

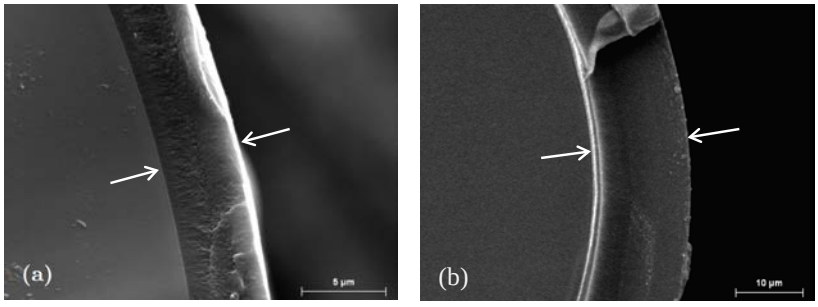

Fig. 1. Scanning electron microscope image of CF1 (a) and CF2 (b).

2. Experimental results and discussion

We tested two polyimide-coated telecom fibers with different coating thickness of 4.5 μm (CF1) and 14 μm (CF2). Scanning electron microscope images of the polyimide coating layers are shown in Fig. 1. For comparison purposes, we repeated the experiments with the same two fibers after removing the coating with sulphuric acid. Hereafter, we will refer to them as BF1, and BF2, respectively. The fiber length used in all cases was 50 cm, approximately. Flexural waves were generated by a piezoelectric transducer coupled to the fibers with an aluminum horn. The piezoelectric transducer was provided by Morgan Advanced Ceramics and consisted on a disc of 1 mm thickness made of PZT-5H, whose nominal thickness mode resonance frequency was 2 MHz. It was driven by an amplified harmonic RF signal supply. No RF impedance matching circuit was used.

Figures 2(a) and 2 (b) shows an example of the transmission spectra obtained. Notches appear at the wavelengths at which the fundamental LP_{01} core mode and different LP_{1m} cladding modes are phase-matched. Notice that the refractive index perturbation introduced by a flexural wave is asymmetric at the cross section of the fiber. Hence, only coupling to LP_{1m} modes is enabled. A detailed analysis about the theoretical basis of modal coupling with flexural waves can be found, for instance, in [17]. Coupling efficiency figures better than 90% were achieved in both fibers. Figure 2(c) shows the deepest notch in the C-band obtained in the experiments with the fiber coated with the thickest polyimide layer, showing a coupling efficiency higher than 93%. We believe that the coupling efficiency in our experiments was limited by the acoustic power able to be delivered to the fiber, thus, we believe that better coupling efficiencies could be achieved if the acoustic wave generation is optimized. In this sense, the use of an impedance matching circuit and/or coaxial horns in conjunction with shear piezoelectric plates can be of interest.

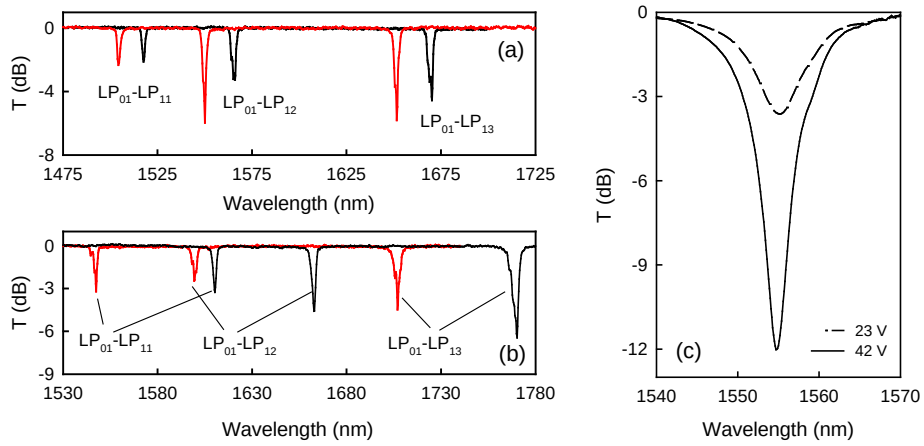

Fig. 2. Transmission spectra showing different mode couplings. Red line is for polyimide-coated fibers and black line is for bare fibers. (a) CF1 and BF1, (b) CF2 and BF2. Frequency of the acoustic wave: 2.06 MHz. (c) LP_{01}-LP_{12} coupling notch for the polyimide coated CF2 fiber and two different RF voltage amplitudes. Frequency of the acoustic wave: 2.25 MHz

Figure 3 shows the resonance wavelength tuning response of the lower order couplings for the two fibers, with and without polyimide coating. In all cases, the resonance wavelength decreases as the frequency of the acoustic wave increases. Notice that the resonance wavelengths of the two bare fibers are shifted. The two fibers were drawn from different preforms, so they have similar but not identical characteristics (see table 1). The notches of

the polyimide-coated fibers are shifted to shorter wavelengths compared to the bare fibers, being the shift larger in the case of CF2 (thicker polyimide coating). Additionally, in both fibers the resonance wavelength blue-shift is larger as the order of the cladding mode involved in the coupling is higher. As an example, at 2.2 MHz, the LP_{01}-LP_{11}, LP_{01}-LP_{12}, and LP_{01}-LP_{13} resonant couplings for fiber CF1 are shifted with respect to its bare fiber counterpart in -14 nm, -16.5 nm and -18.9 nm, respectively, while for fiber CF2 the resonances are shifted in -39 nm, -53.3 nm, and -63 nm.

We found that the main contribution to such blue-shift comes from the dispersion relation of the flexural acoustic wave. Using a fiber optic vibrometer [18], we measured the acoustic wavelength of the flexural elastic mode, as a function of frequency. Figure 4 shows the result for fibers CF2 and BF2. It is shown that, for all frequencies, the acoustic wavelength was shorter in the polyimide-coated fiber than in the bare fiber counterpart. In this particular case, the relative acoustic wavelength change is about -0.055, and it is rather constant over this frequency range. In the case of CF1, the changes in the dispersion of the flexural mode introduced by the thin polyimide layer with respect to the bare fiber were significantly smaller, and comparable to the accuracy of our experimental arrangement. So, we were not able to resolve properly the differences between the acoustic wavelength in CF1 and BF1.

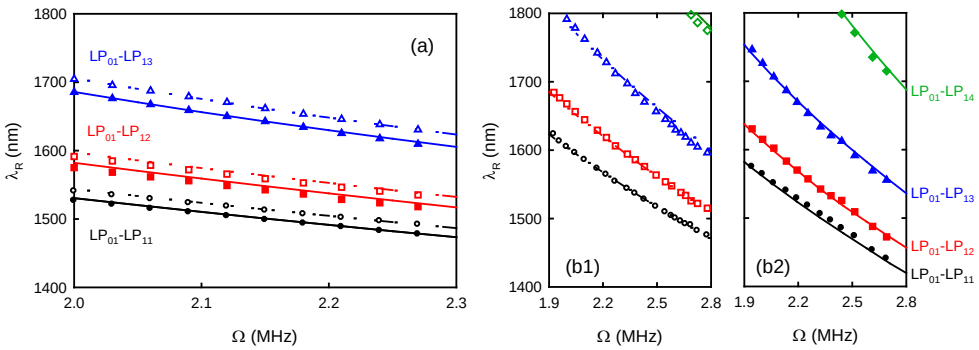

Fig. 3. Resonance wavelength tuning with acoustic frequency for the polyimide-coated fibers (closed symbols) and the bare fibers (open symbols). (a) Fibers CF1 and BF1, (b1) fiber CF2 and (b2) fiber BF2. The lines show theoretical calculations. Dashed lines are for bare fibers and solid lines for the polyimide-coated fibers.

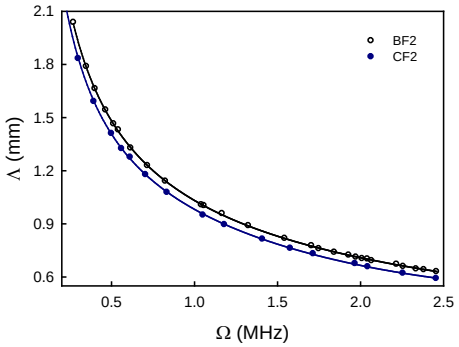

Fig. 4. Experimental characterization of the dispersion relation of the flexural elastic wave propagating along the polyimide-coated fiber CF2 (red) and the bare fiber BF2 (black). Symbols are experimental data and lines are theoretical calculations following [19].

In the low-frequency regime, the dispersion relation of the fundamental flexural mode in a cladded solid cylinder can be expressed as [19]:

$$\Lambda = \left(\frac{\pi}{\Omega}\right)^{1/2} \left[\frac{E_1 a^4 + E_2 \left(b^4 - a^4\right)}{\rho_1 a^2 + \rho_2 \left(b^2 - a^2\right)}\right]^{1/4} \quad (1)$$

where E_1, ρ_1 *and* E_2, ρ_2 are the Young modulus and mass density of the inner cylinder and the coating, respectively, and a and b are the inner and outer radius. Taking into account the values for the material parameters for silica and polyimide that can be found in the literature (E_1=73.1 GPa, E_2=3 GPa, ρ_1=2200 kg/m^3, ρ_2=1430 kg/m^3), the relative wavelength change calculated using Eq. (1) for a 125 μm diameter fiber with a polyimide coating of 14 μm thickness is 0.056, which is in good agreement with the experimental measurements.

We calculated the resonance wavelength, λ_R, for the different couplings in both fibers. According to the coupling mode theory [20], λ_R, is given by:

$$\lambda_R = \Delta n_{eff} \cdot \Lambda \quad (2)$$

where Λ is the acoustic wavelength, and Δn_{eff} is the effective index difference between the two optical modes. The modal effective indices were calculated using a three-layer step-index model (core/cladding/outer medium). In the cases of CF2 and the two bare fibers (BF1, and BF2), the acoustic wavelength as a function of frequency was obtained from the experimental measurements shown in Fig. 3. In the case of fiber CF1, the correction to the acoustic wavelength introduced by the presence of the polyimide coating was estimated from Eq. (1) (relative acoustic wavelength change of 0.019 with respect to the bare fiber). In a first step, we found the fiber parameters, i.e., NA, cutoff wavelength (λ_c), and outer diameter (OD) that led to the best fit of the resonance wavelengths for the two bare fibers. The result of these calculations are include in Fig. 3. The fiber parameters that resulted from this fitting process, as well as the nominal values are given in table 1. Good agreement is obtained for NA and outer diameter, however the cut-off wavelength obtained experimentally is larger than the nominal value. This discrepancy was already reported previously and it is related to the fact that the nominal value provided by the manufacturer is a practical parameter but it is not exactly the electromagnetic cutoff wavelength of the LP_{11} mode [10]. Then, we calculated the resonance wavelengths for the two polyimide-coated fibers just taking into account the corresponding change in the acoustic wavelength. The results are included in Fig. 3. The calculations are in good agreement with the experimental data. Notice that the influence of the refractive index of the outer polyimide layer on the modal index of the cladding modes has been neglected in this calculation. Thus, we can conclude that the resonances' shift is mainly due to the modification of the acoustic properties of the fiber because of the polyimide jacket.

A comparison of the acousto-optic coupling efficiency in the different fibers was carried out. Figure 5(a) gives the depth of the LP_{01}-LP_{11} coupling notch obtained with fibers CF1, CF2, and BF1, as a function of the voltage applied to the piezoelectric transducer. The results obtained for BF2 were pretty similar to BF1, and for simplicity they are not included. Care was taken to perform the three experiments under similar conditions (we used the same piezoelectric, same frequency, and followed identical fiber-to-horn attachment procedures in all cases). The best efficiency was achieved with the bare fiber. However, we would like to remark that the performance of CF1 is just slightly inferior to the result for the bare fiber. At the highest voltage, the coupling efficiency achieved for CF1, CF2, and BF1 were 92 %, 67%

and 94%, respectively. Notice that the resonance coupling that we compare in this experiment (LP_{01}-LP_{11}) is the one with the lowest coupling coefficient [17, 20].

Table 1. Optical characteristics of the fibers. Nominal and best-fit parameters.

	Nominal values			*Best-fit values*		
Fiber	***λ_c (μm)***	***NA***	***OD (μm)***	***λ_c (μm)***	***NA***	***OD (μm)***
CF1/BF1	1.20	0.12	125	1.30	0.12	125
CF2/BF2	1.27	0.12	125	1.37	0.12	125

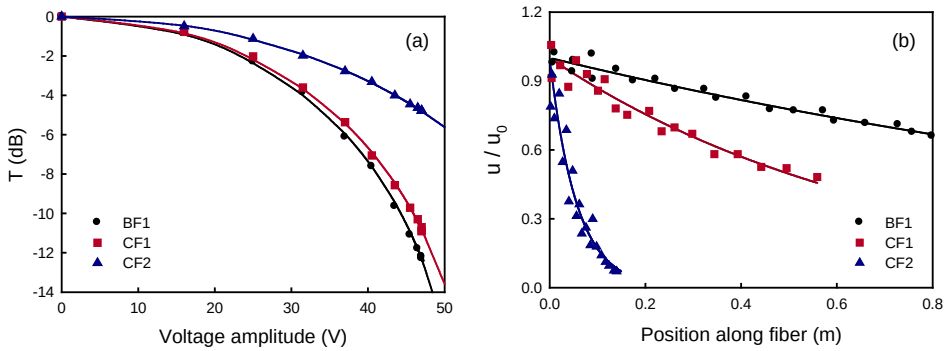

Fig. 5. (a) Comparison of LP_{01}-LP_{11} notch depth vs. voltage, for fibers CF1, CF2 and BF1. Symbols are experimental data and lines are the best fit to theoretical transmittance. Frequency: 2.217 MHz. (b) Normalized amplitude of the acoustic wave along the fibers. U_0 is the amplitude at the excitation point. Symbols are experimental data and lines are the best fit to an exponential decay function.

The differences in coupling strength among the three fibers are caused by the attenuation of the elastic wave. Using an optical vibrometer, we measured the amplitude decay of the acoustic wave along a section of each fiber. The experimental data are shown in Fig. 5(b) for a frequency of 2.1 MHz, along with fitted exponential decay functions. The attenuation factors found are 0.51 m^{-1} for the bare fibers, and 1.42 m^{-1}, and 17.7 m^{-1}, for CF1 and CF2, respectively. In practical terms, the attenuation of the acoustic wave causes the acousto-optic interaction effective length to be much shorter than the actual physical length. Given the attenuation factors obtained, the effective length is limited to about 70 cm for CF1 and 5 cm for fiber CF2.

The limitation on the effective interaction length imposed by the attenuation, can also affect the 3-dB bandwidth of the notches, which depends, among other parameters, on the interaction length: the longer is interaction length, the narrower are the resonances. In the case of CF1, it can be much longer than the typical interaction lengths considered in practical implementations. Then, we can conclude that notches in this polyimide-coated fiber could be as narrow as in its bare fiber counterpart. However, in the case of CF2 where the effective interaction length is limited to just 5 cm, it can certainly be a limitation when very narrow

notches are wanted. In summary, the present results for fiber CF1 give notch depth and 3-dB bandwidth similar to those reported in other fiber-integrated devices [1-4], while in the case of fiber CF2, the notch depth is lower and the 3-dB bandwidth can be limited because of the reduced maximum interaction length.

3. Conclusions

Acousto-optic coupling in polyimide-coated single-mode optical fibers using flexural waves is reported for the first time. The polyimide coating modifies significantly the acoustic properties of the fiber with respect to the bare fiber counterpart. The acoustic wavelength dispersion and the attenuation of the elastic wave were characterized in detail. The blue-shift of the acousto-optic resonances is successfully explained as a result of the acoustic wavelength change. The elastic attenuation increases significantly with the polyimide layer thickness. Taking into account the measured attenuation factors, we have estimated the longest effective interaction length possible, in about 70 cm for the fiber with 4.5 μm coating thickness and 5 cm for the fiber with 14 μm thickness. Coupling efficiency > 93 % is demonstrated in the C-band with the fiber coated with the thickest polyimide layer. Acousto-optic coupling in polymide-coated fibers using other type of elastic waves, as longitudinal waves, is expected to be also feasible.

Funding

Agencia Estatal de Investigación (AEI) of Spain and Fondo Europeo de Desarrollo Regional (FEDER) (Ref.: TEC2016--76664-C2-1-R); Generalitat Valenciana (Ref.: PROMETEOII /2014/072).